Targeting Radiation-Resistant Prostate Cancer Stem Cells by B7-H3 CAR T Cells

Yida Zhang[1,2], Lile He[1], Ananthan Sadagopan[1], Tao Ma[1], Gianpietro Dotti[3], Yufeng Wang[1], Hui Zheng[4], Xin Gao[5], Dian Wang[6], Albert B. DeLeo[1], Song Fan[1], Ruochuan Sun[1], Ling Yu[1], Liyuan Zhang[1], Gongxian Wang[2], Soldano Ferrone[1,7], and Xinhui Wang[1]

ABSTRACT

Radiotherapy (RT) is a key treatment for prostate cancer. However, RT resistance can contribute to treatment failure. Prostate cancer stem cells (PCSCs) are radioresistant. We recently found that fractionated irradiation (FIR) upregulates expression of the immune checkpoint B7-H3 (CD276) on PCSCs and bulk cells in each prostate cancer cell line tested. These findings prompted us to investigate whether B7-H3 targeting chimeric antigen receptor (CAR) T cells, which may abrogate function of an immune checkpoint and mediate lysis of targeted cells, can target RT-resistant PCSCs *in vitro* and *in vivo*. B7-H3 expression is naturally higher on PCSCs than bulk prostate cancer cells and cytotoxicity of B7-H3 CAR T cells to PCSCs is more potent than to bulk prostate cancer cells. Furthermore, FIR significantly upregulates B7-H3 expression on PCSCs and bulk prostate cancer cells. The duration of FIR or single-dose irradiation-induced further upregulation of B7-H3 on bulk prostate cancer cells and PCSCs lasts for up to 3 days. B7-H3 CAR T-cell cytotoxicity against FIR-resistant PCSCs at a low effector to target ratio of 1:1 was assessed by flow cytometry and sphere formation assays. Further upregulation of B7-H3 expression by FIR made PCSCs even more sensitive to B7-H3 CAR T-cell–mediated killing. Consequently, the FIR and B7-H3 CAR T-cell therapy combination is much more effective than FIR or CAR T cells alone in growth inhibition of hormone-insensitive prostate cancer xenografts in immunodeficient mice. Our work provides a sound basis for further development of this unique combinatorial model of RT and B7-H3 CAR T-cell therapy for prostate cancer.

Significance: We demonstrate that FIR significantly upregulates B7-H3 expression by RT-resistant PCSCs and bulk cells; cytotoxicity of B7-H3 CAR T cells to FIR-treated PCSCs is potent and results in significantly improved antitumor efficacy in mice.

Introduction

Prostate cancer is the most common noncutaneous cancer among American men with an estimated 191,930 new cases in 2020 and the third highest cause of cancer deaths in the United States, with an estimated 33,330 deaths (1). Organ-confined prostate cancer is typically treated with surgery and/or radiotherapy (RT), the latter given as brachytherapy or external beam RT (2). Specifically, RT alone or RT in combination with androgen deprivation therapy is commonly recommended to treat patients after prostatectomy with high-risk features such as extracapsular extensions, positive surgical margins, or persistent/rising prostate-specific antigen levels, as well as newly diagnosed patients with low-volume metastatic disease (3). However, RT is associated with a biochemical recurrence rate of 20% to 30% in patients with organ-confined prostate cancer and is unlikely to be curative for patients with locally advanced disease or multiple high-risk features post-prostatectomy (4, 5). Resistance to RT contributes to prostate cancer recurrence and mortality (6) and subclinical micrometastases present at diagnosis contribute to early biochemical failure and distant metastasis (7). This clinical challenge underscores the urgency to develop therapies more effective than those currently available for patients with prostate cancer.

Considerable evidence indicates that cancer treatment resistance and recurrence is due to cancer stem cells (CSCs), a small subpopulation of tumor cells present in the bulk tumor and/or metastases, which have "stem cell–like" properties, including chemo- and radioresistance (8, 9). These CSCs have been identified and isolated from a wide range of human tumors, including prostate cancer (8–12). Like other human CSCs studied, human prostate CSCs (PCSCs) have been shown in animal tumor model systems to have high tumorigenicity in immunodeficient mice and metastatic potential (10).

Cancer immunotherapy has been successfully applied clinically to a number of cancer types, including prostate cancer. The dendritic cell vaccine therapy sipuleucel-T has been approved since 2010 for treatment of patients with metastatic castration-resistant prostate cancer (13), and ongoing clinical trials are evaluating additional immunotherapies, such as immune checkpoint inhibitors and adoptive cell therapies (14). Indeed, all elements of the host's immune system are now being clinically employed in various forms of passive and active immunotherapeutic protocols. One of the most innovative approaches combines antibody fragments with T-cell–based immunology to target cancer cells, namely, the development of genetically engineered chimeric antigen receptor (CAR) T cells (15). By combining the tumor

[1]Division of Surgical Oncology, Department of Surgery, Massachusetts General Hospital, Harvard Medical School, Boston, Massachusetts. [2]Department of Urology, The First Affiliated Hospital of Nanchang University, Nanchang, Jiangxi, China. [3]Lineberger Comprehensive Cancer Center and Department of Microbiology and Immunology, University of North Carolina, Chapel Hill, North Carolina. [4]Biostatistics Center, Massachusetts General Hospital, Harvard Medical School, Boston, Massachusetts. [5]Division of Hematology/Oncology, Department of Medicine, Massachusetts General Hospital, Harvard Medical School, Boston, Massachusetts. [6]Department of Radiation Oncology, Rush University Medical Center, Chicago, Illinois. [7]Department of Orthopaedic Surgery, Massachusetts General Hospital, Harvard Medical School, Boston, Massachusetts.

Note: Supplementary data for this article are available at Molecular Cancer Therapeutics Online (http://mct.aacrjournals.org/).

L. He and A. Sadagopan have contributed equally to this article.

Corresponding Author: Xinhui Wang, Massachusetts General Hospital, 55 Fruit St, Boston, MA 02114. Phone: 617-726-7881; Fax: 617-726-8623; E-mail: xwang30@mgh.harvard.edu

Mol Cancer Ther 2021;20:577–88

doi: 10.1158/1535-7163.MCT-20-0446

antigen (TA) epitope recognition of an antibody fragment with the properties of a T-cell receptor, the CAR T cell has the potential to recognize tumor-associated/specific molecules presented on the tumor cell surface and induce the cytolytic activity of a T cell to mediate tumor cell lysis.

To date, however, CAR T-cell therapy has demonstrated enhanced antitumor activity against blood cancers compared with solid tumors (16). Although anti-CD19 and anti-CD22 CAR T-cell therapy for leukemia have been successful overall, treatment failures due to low levels of antigen expression as well as immunoselection of epitope loss variants are common (17, 18). In addition, the challenges for successful application of CAR T-cell therapy for solid tumors include the increased heterogeneity of solid tumors relative to leukemias, identifying suitable high-density antigenic targets, and migration of antitumor T cells, especially adoptively transferred immune effector cells, into the hostile tumor microenvironment, which can reduce their persistence and functionality.

Currently, three tumor-associated antigens have been targeted in clinical trials of CAR T-cell therapy for patients with metastatic prostate cancer. In general, patients in these trials have not responded beneficially to any significant degree to CAR T-cell therapy against the prostate-specific membrane antigen (PSMA) and prostate stem cell antigen (PSCA) (19). Clinical trials targeting the third TA, the epithelial cell adhesion molecule (EPCaM), with CAR T cells are currently being conducted and evaluated for several cancers, including prostate cancer (19). However, as noted above, one challenge in making a CAR T-cell therapy effective for prostate cancer is the choice of the targeted TA. For instance, PSCA is not expressed on all prostate cancer (20) and PSMA is expressed in brain tissue, which raises the possibility of serious therapy complications (21). Further understanding and selection of cancer TAs has significant potential to strengthen the effectiveness of CAR T-cell–based prostate cancer therapy.

In recent years, the development of various classes of agents having the ability to enhance T-cell–based antitumor immune responses by blocking immune checkpoints has greatly contributed to the increased clinical application of tumor immunotherapy (22). Tumor cells express immune checkpoints, which interact with cytotoxic T lymphocytes (CTLs) and block the ability of these effectors to mediate cytolysis of the targeted tumor cells. B7-H3 is an immune inhibitory molecule expressed at elevated levels in a large number of cancer types, including pancreatic ductal adenocarcinoma (PDAC), ovarian cancer, lung cancer, clear cell renal carcinoma and prostate cancer (15, 23). In prostate cancer, elevated expression level of B7-H3 is associated with high Gleason score, advanced stage, metastases, and poor patient prognosis (23, 24). Clinical targeting of B7-H3 with the mAb enoblituzumab has resulted in tumor regression in patients with treatment-refractory prostate cancer (25). Recent studies have found strong evidence that B7-H3 regulates T-cell–mediated immune response and inhibition of B7-H3 results in T-cell proliferation (26, 27). Moreover, blocking activated T cells with a bispecific anti-CD3 x anti-B7-H3 antibody enhanced T-cell cytotoxicity and increased cytokine production of IFNγ, TNFα, and IL2 (28). Crucially, B7-H3 expression is minimal in healthy tissue (26).

This study focuses on the development of a CAR T-cell therapy targeting the immune checkpoint B7-H3, which is expressed on PCSCs and bulk prostate cancer cells. The B7-H3 CAR T cells used in this study are expected to be bifunctional; they can abrogate function of the B7-H3 immune checkpoint and mediate lysis of targeted tumor cells. The anti-B7-H3 CAR construct was derived from the single-chain variable fragment (scFv) of the B7-H3-specific 376.96 mAb (15) and already has demonstrated significant and persistent cytolytic activity against PDAC, ovarian cancer, and neuroblastoma in previous studies (15).

Combinatorial approaches have led to multiple recent successes in the treatment of advanced prostate cancer and other cancers (29–31). The aim of this study was to evaluate the efficacy of B7-H3 CAR T-cell therapy against RT-resistant prostate cancer. The CAR T cells were used as a monotherapy or in combination with FIR against two human prostate cancer cell lines, DU145 and PC3, in *in vitro*- and *in vivo*-based preclinical experiments with particular emphasis on evaluating the targeting of FIR-resistant PCSCs, which are responsible for tumor formation, progression and metastasis and thus may be responsible for treatment failure and mortality (10–12).

Materials and Methods

Cell lines and cell culture

The human prostate cancer cell lines DU145 and PC3, and the human Burkitt's lymphoma cell line Raji were purchased from the ATCC. The human breast cancer cell line SUM159 was obtained from Asterand Bioscience Inc., and the SUM159 B7-H3 knockout (KO) cell line was generated by CRISPR-Cas9 Knockout Kit (Catalog No. sc-402032; Santa Cruz Biotechnology) in our laboratory. All the cell lines were cultured in RPMI1640 medium (Corning Incorporated) supplemented with 2 mmol/L L-glutamine (Corning) and 10% FBS (Gemini Bio-Products LLC) at 37°C in a 5% CO_2 humidified atmosphere.

Animals

Eight-week-old, male NSG mice were obtained from the Massachusetts General Hospital COX7 animal facility. The Institutional Animal Care and Use Committee has approved all the animal studies.

FIR or single-dose irradiation

In vitro, cells plated in 6-well plates (Corning) at a density of 5×10^5 cells/well in 2-mL RPMI1640 medium containing 10% FBS were irradiated with a single dose of irradiation (IR) [0, 2, 6, 10, 16, or 20 Gray (Gy)] or FIR (2 Gy/daily for 3 or 5 days). *In vivo*, FIR at 4 Gy/daily was delivered locally at the indicated fractions to each mouse tumor area while the remaining body was covered by a lead shield. The X-RAD 320 Biological Irradiator (Precision X-ray Inc.) was used for all *in vitro* and *in vivo* experiments.

Identification of $ALDH^+CD44^+$ PCSCs

Tumor cells were stained using the ALDEFLUOR (Stem Cell Technologies) and anti-human CD44 (clone No. G44-26; Miltenyi Biotec Inc.). The $ALDH^+CD44^+$ PCSCs were detected by flow cytometry using a BD Accuri C6 flow cytometer (BD Biosciences) and sorted using a FACS Aria II Cell Sorter Flow Cytometer (BD Biosciences) (32).

Generation of B7-H3 CAR T cells

Peripheral blood mononuclear cells (PBMCs) were isolated from normal human donor blood (Research Blood Components) with Lymphoprep (Stem Cell Technologies). On day 0, the PBMCs (1×10^6/well) were activated in a nontreated 24-well cell culture plate (#351147; Corning) precoated with 1 μg/mL CD3 (clone OKT3; Miltenyi Biotec) and 3 μg/mL CD28 antibodies (clone CD28.2; BD Biosciences) in the complete medium [45% RPMI1640 and 45% Click's medium (Irvine Scientific), 10% FBS, 1% Penicillin, and 1% Streptomycin (Corning)]. On day 1, activated T cells were expanded by addition of IL7 (10 ng/mL, PeproTech) and IL15 (5 ng/mL, PeproTech; CAR T medium). On day 2, the activated and expanded T cells were

transferred to wells of 24-well plates that had been previously coated with RetroNectin (Takara Bio Inc.) and contained retroviral particles of the B7-H3 CAR construct (15). On day 4, to allow for their continued expansion, the transduced cells were collected and transferred to tissue culture-treated 24-well plates (Catalog No. 353047; Corning) with each well containing 0.5 mL of the activated T-cell suspension (5×10^5 cells/well) and 1.5 mL of fresh CAR T medium. On day 6, an aliquot of transduced cells was analyzed for transduction efficiency and 50% CAR T spent medium was replaced with fresh medium, that is, 50:50 (v/v) old medium: new medium. On day 8, CAR T cells were counted and reseeded at 1×10^6/well in 2 mL of fresh CAR T medium to further expand cells. On day 10, 50% spent medium was replaced with the fresh medium as done on day 6. On day 13 to 14, CAR T cells and nontransduced T (NT) cells grown at similar conditions were collected, aliquoted, and frozen for storage in a liquid nitrogen freezer for *in vitro* and *in vivo* experiments.

Flow cytometry analysis

PC3, DU145, Raji, and SUM159 B7-H3 KO cells (10^7 cells) were stained with the human B7-H3 specific mouse mAb 376.96 (1 μg/mL) for 30 minutes at 4°C and washed twice with 0.5% BSA/PBS using mouse mAb F3C25 as isotype control (33). Cells were then stained with R-Phycoerythrin AffiniPure F(ab')$_2$ Fragment Goat Anti-Mouse IgG (H+L; Jackson ImmunoResearch Inc.; 1:100) as the secondary antibody for 30 minutes at 4°C and washed twice with 0.5% BSA/PBS. Cell surface expression of the scFv of mAb 376.96 on CAR T cells was determined by incubating the cells with 10% human AB serum/PBS (Catalog No. HP1022HI; Valley Biomedical Products and Services Inc.) for 15 minutes, followed by two washes with 0.5% BSA/PBS and staining with recombinant human B7-H3 Fc Chimera Protein, CF (R&D Systems) and then R-Phycoerythrin AffiniPure F (ab')$_2$ Fragment Goat Anti-Human IgG, Fcγ fragment specific antibodies (Jackson ImmunoResearch), and APC-Cy7 Mouse Anti-Human CD3 mAb (Clone SK7; BD Biosciences). The phenotype of CAR T-cell surface antigens was determined by staining the cells with PE/Cyanine7 anti-human CD3 (clone UCHT1), FITC anti-human CD4 (clone A161A1), APC/Cyanine7 anti-human CD8 (clone SK1), APC anti-human CD45RA (clone HI100), and PE anti-human CD62L (clone DREG-56) antibodies. All these reagents were purchased from BioLegend Inc., and the cells were analyzed by flow

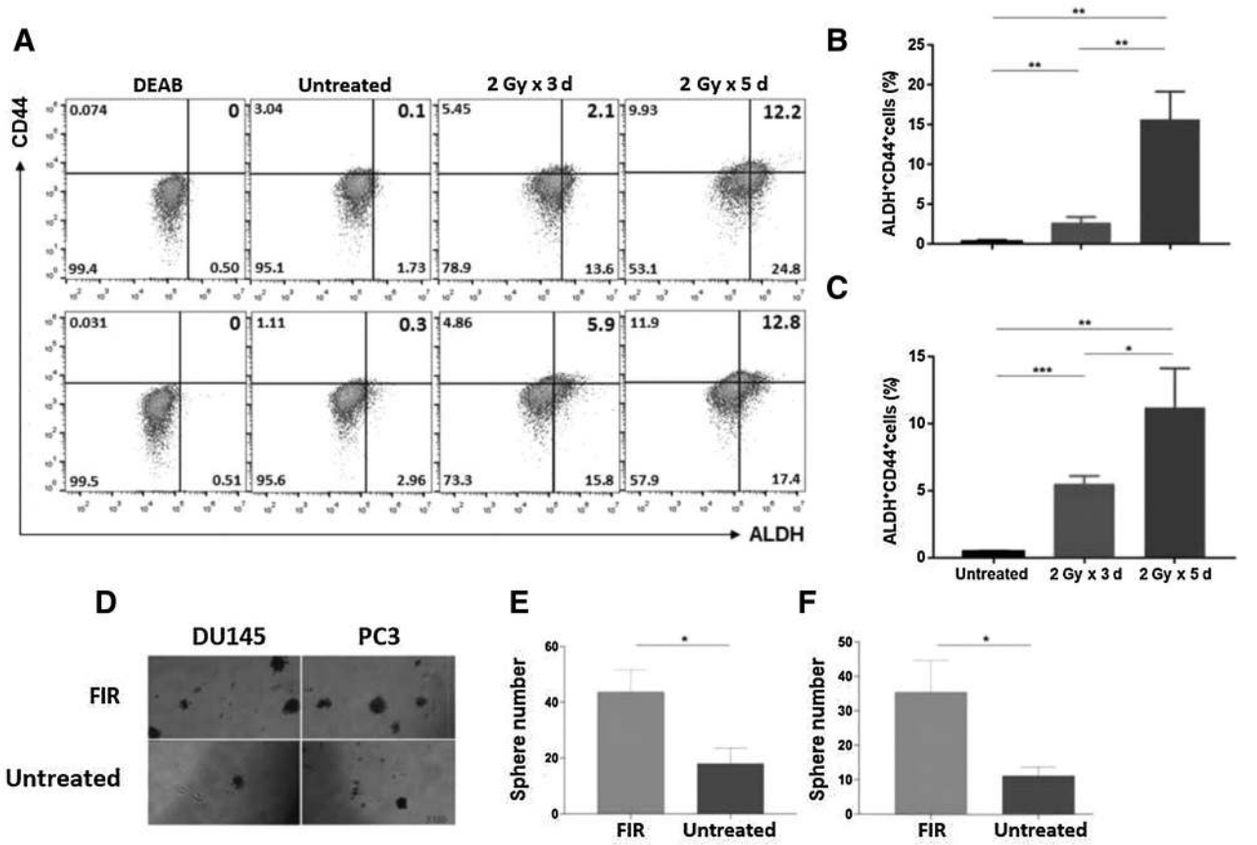

Figure 1.

PCSCs are FIR-resistant. Prostate cancer cells were irradiated at doses and times as indicated, and after 24 hours analyzed for $ALDH^+CD44^+$ cells by flow cytometry. Data are shown for DU145 (**A**, top) and PC3 (**A**, bottom) cell lines. $ALDH^+CD44^+$ PCSCs (%) are presented in the upper right quadrant. DEAB, an inhibitor of ALDH1/3 isoforms, was used to establish the baseline fluorescence as the gating reference standard of $ALDH^-$ population. Mean± SD of $ALDH^+CD44^+$ cells (%) are shown for cell lines DU145 (**B**) and PC3 (**C**). Cells plated in 6-well cell culture plates (Corning) at a density of 5×10^5 cells/well in 2-mL RPMI1640 medium containing 10% FBS were treated with FIR (2 Gy/day x 5 days). Cells were trypan blue stained to exclude dead cells and living cells were tested for their ability to form spheres. After 7 to 10 days, small spheres were detected by microscopy. At day 18, spheres/well were counted. Representative photographs of DU145 and PC3 cells lines are shown (100×; **D**) as well as mean ± SD of spheres/well for DU145 (**E**) and PC3 (**F**). The experiments were repeated three times (*, $P < 0.05$; **, $P < 0.01$; ***, $P < 0.001$).

cytometry using the LSR II cytometer (BD Biosciences) and FlowJo software.

Clonogenic assay

DU145 and PC3 prostate cancer cells were seeded into 6-well plates at a density of 5×10^5 cells/well and cultured in the regular cell culture medium overnight at 37°C in a 5% CO_2 humidified atmosphere. Cells were irradiated with 2 Gy/day for either 3 or 5 days and incubated for 10 to 14 days under previously described conditions. Colonies composed of 50 cells or more were counted as described previously (8).

Apoptosis assay

Apoptotic cells were detected using FITC Annexin V Apoptosis Detection Kit with 7-AAD (BioLegend). FIR-treated cells were collected, washed, resuspended at a cell density of 10^6 cells/500 μL of 1X binding buffer, and stained with 5 μL of Annexin V-FITC and 5 μL of 7AAD at RT for 15 minutes in the dark. A minimum of 10,000 cells within the properly gated region was analyzed for apoptosis by flow cytometry (32).

Sphere formation assay

Nonnecrotic tumor tissue specimens harvested from xenograft-bearing NSG mice were collected at the time of sacrifice and a single cell suspension was obtained as described previously (9). Cultured tumor cells treated with FIR or co-cultured with CAR T cells, or single cell suspensions of xenograft tumors were seeded (300 cells/well) in triplicate wells in 24-well ultra-low attachment plates (Corning) in sphere formation medium as described previously (9).

In vitro cell cytotoxicity assays

Target cells (5,000 cells/well) were plated in 96-well plates (Catalog No. 353072; Corning) in 100 μL of complete growth medium and grown overnight. B7-H3 CAR T cells were added to the wells the next day at the indicated effector to target (E:T) ratios and cultured for 48 hours at 37°C in a 5% CO_2 humidified atmosphere. T cells were removed by washing with PBS. The targeted tumor cells were quantified by a viable cell MTT assay, as described previously (34) or co-cultured cells were simultaneously stained for residual tumor cells by B7-H3 specific mouse mAb 376.96 and R-Phycoerythrin AffiniPure F(ab')$_2$ Fragment Goat Anti-Mouse IgG (H+L) and CAR T cells by APC-Cy7 Mouse Anti-Human CD3 and analyzed by a flow cytometer.

In vivo prostate xenograft models

DU145 cells (2×10^6 cells/mouse) or PC3 cells [5×10^6 cells in 50 μL RPMI1640 serum-free medium mixed with 50-μL Matrigel (Corning)/mouse] were implanted subcutaneously using a 22-gauge needle (BD Biosciences) in the right thighs of NSG mice. Body weight and tumor volume were measured every 3 days. Treatments were initiated when the tumors had an approximate diameter of 50 mm^3. Mice were divided into groups using a stratified randomization strategy ($n = 5$ mice/group), such that the difference of mean tumor volumes was not statistically significant between each group. FIR (4 Gy/day) was delivered to the local tumor area at indicated times. A single treatment with B7-H3 CAR T cells or NT cells (10^6 cells/mouse) was given through tail–vein injection at different specified times. Mice were left untreated as controls. Tumor volumes were measured by digital caliper and calculated by the formula: volume $= 1/2 \times$ length $\times$ width^2.

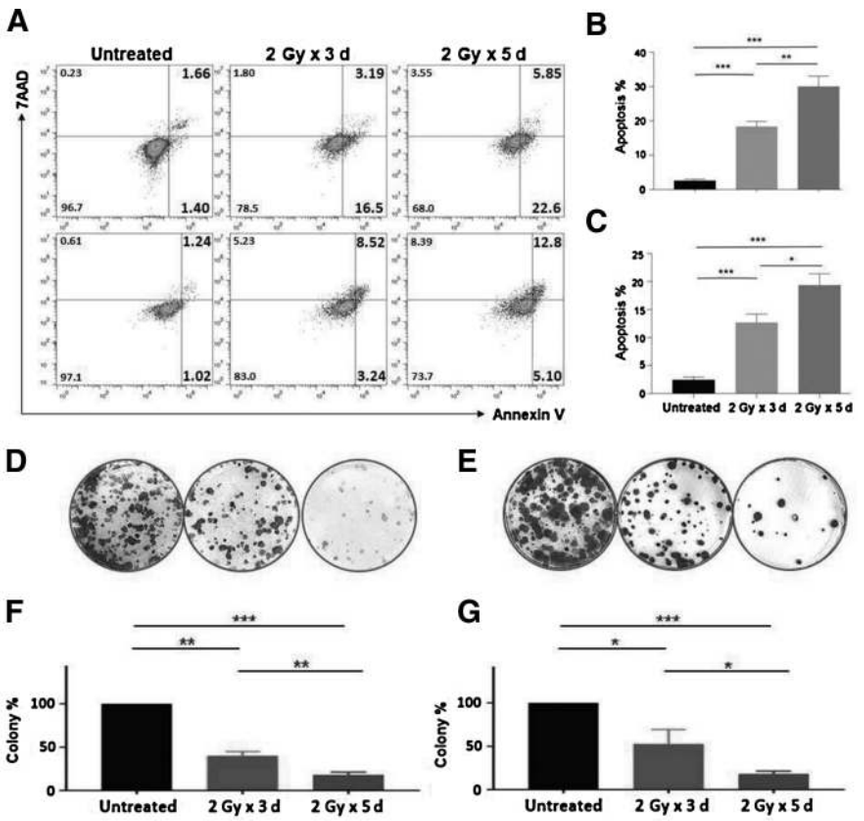

Figure 2.

Prostate cancer cells are resistant to FIR-induced apoptosis. Prostate cancer cells were irradiated at doses and times as indicated, and 24 hours later were assessed for apoptosis using Annexin V/7-AAD staining. Data for DU145 (**A**, top) and PC3 (**A**, bottom) cell lines are shown. Annexin V$^+$ apoptotic cells (%) are presented in the right quadrants. Mean ± SD of apoptotic cells (including 7AAD+ late apoptotic or necrotic cells, %) are shown for DU145 (**B**) and PC3 (**C**) cell lines. The irradiated cells were trypan blue stained to exclude dead cells, and living cells were tested for their ability to form colonies. At day 12, colonies/well were counted. The colonies in untreated wells were too numerous and set as 100%. Representative pictures of DU145 (**D**) and PC3 (**E**) and mean ± SD of colonies (%) for DU145 (**F**) and PC3 (**G**) are shown. The experiments were repeated three times (*, $P < 0.05$; **, $P < 0.01$; ***, $P < 0.001$).

The dose of FIR was chosen because it is between clinical moderate hypofractionation (2.4–3.4 Gy/fraction) and ultrahypofractionation (≥5 Gy/fraction) (35).

Immunofluorescence staining of frozen prostate cancer xenograft tissue sections

Optimal cutting temperature compound (OCT)-embedded frozen xenograft tissue blocks were sectioned by a microtome-cryostat into 4- to 5-μm-thick tissue slides. These tissue slides were stained by primary mAb 376.96 (0.1 μg/mL) and detected with the Goat Anti-Mouse IgG (H+L) Highly Cross-Adsorbed Secondary Antibody, Alexa Fluor Plus 594 (diluted at 1:500; Catalog No. A32742; Thermo Fisher Scientific). Cell nuclei were counterstained with DAPI.

Statistical methods

A two-tailed Student *t* test or a one-way ANOVA with Tukey HSD *post hoc* tests were performed to interpret the differences between experimental and control groups. All *in vitro* experiments were conducted three times. Differences in B7-H3 CAR T-cell–mediated cytotoxicity on different cell populations (including all three E:T ratios) were detected using a chi-square test in a two-way ANOVA. Differences between tumor volumes were analyzed by chi-square test in an ANOVA with repeated measurements. The above models were fitted using SAS version 9.4 (SAS Institute, Inc.).

Results

PCSCs are resistant to FIR

It has been known that PCSCs are resistant to irradiation (IR) (36, 37). Moreover, IR induces PCSCs (38). In agreement with the literature, it was determined that PCSCs, defined as $ALDH^+CD44^+$ cells (39), were enriched from 0.35 ± 0.18% to 15.67 ± 3.51% ($P < 0.01$) and from 0.43 ± 0.12% to 11.2 ± 2.95% ($P < 0.01$) in DU145 and PC3 cell lines, respectively, in response to a clinically relevant FIR setting (2 Gy/day × 5 days). In both cell lines, the enrichment of PCSCs was proportional to the total FIR dose (**Fig. 1A–C**). In addition, sphere formation, a common *in vitro* functional marker for identifying CSCs, confirmed the results of the flow cytometry analysis and showed the FIR-resistance of PCSCs. FIR treatment (2 Gy/day x 5 days) increased sphere formation 2.5-fold ($P < 0.05$) and 3.3-fold ($P < 0.05$) in DU145 and PC3 cells, respectively, compared with untreated cells (**Fig. 1D–F**). Relative to untreated cells, FIR induced significantly more apoptotic cells in the bulk cell populations of DU145 (29.87 ± 3.35% vs. 2.37 ± 0.55%) ($P < 0.001$) and PC3 (19.8 ± 2.4% vs. 2.73 ± 0.68%; $P < 0.001$) cell lines, respectively. Induction of apoptosis was dose-dependent. FIR of 2 Gy/day × 3 days induced lower levels of apoptosis than FIR of 2 Gy/day × 5 days in DU145 (17.7 ± 1.66% vs. 29.87 ± 3.35%; $P < 0.01$) and PC3 (12.3 ± 1.51% vs. 19.8 ± 2.4%; $P < 0.05$) cells (**Fig. 2A–C**). Similarly, FIR significantly reduced, but did not eradicate cells in a clonogenic assay, which tested at the single cell level its long-term effects on colony formation of DU145 and PC3 cells (**Fig. 2D–G**).

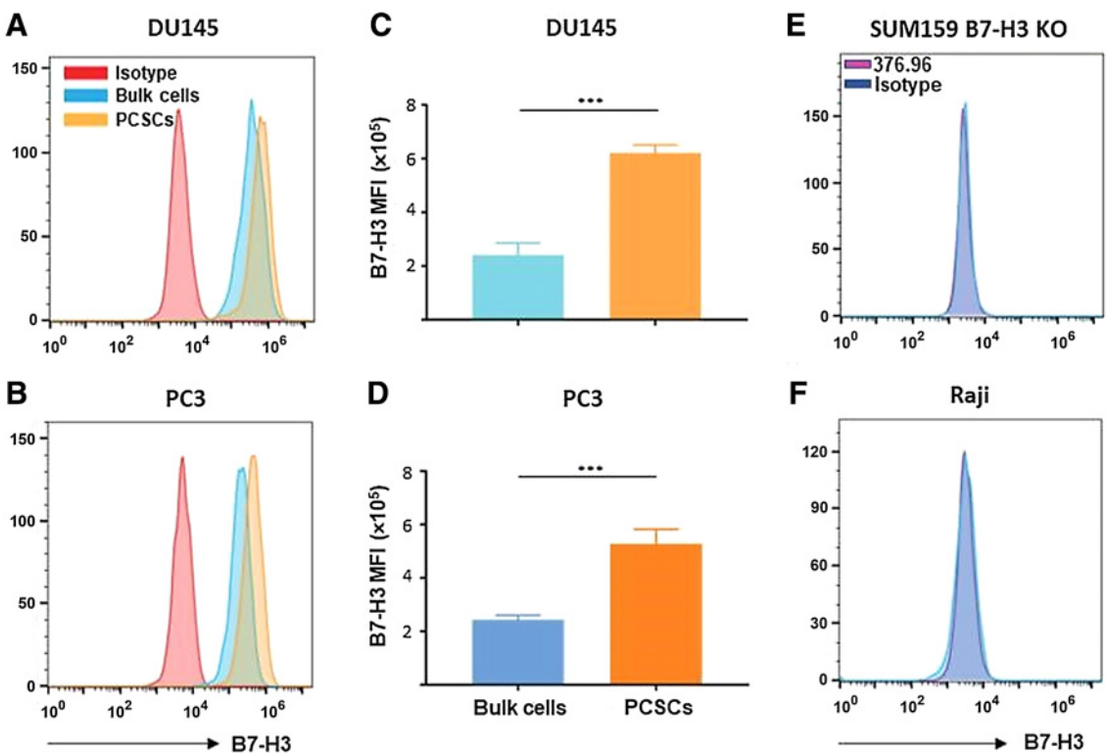

Figure 3.

PCSCs express higher levels of B7-H3 antigen than bulk prostate cancer cells. Sorted $ALDH^+CD44^+$ PCSCs and unsorted bulk cells were stained with B7-H3-specific mAb 376.96 for detection of B7-H3 expression. Flow cytometry histograms of $B7\text{-}H3^+$ PCSCs and bulk cells are shown for DU145 (**A**) and PC3 (**B**) cell lines, as well as mean ± SD of B7-H3 MFI for DU145 (**C**) and PC3 (**D**) cell lines. A mouse IgG2a mAb F3C25 was used as the isotype control. The $B7\text{-}H3^-$ SUM159 B7-H3 KO (**E**) and Raji (**F**) cell lines were used as negative controls. The experiments were repeated three times (***, $P < 0.001$).

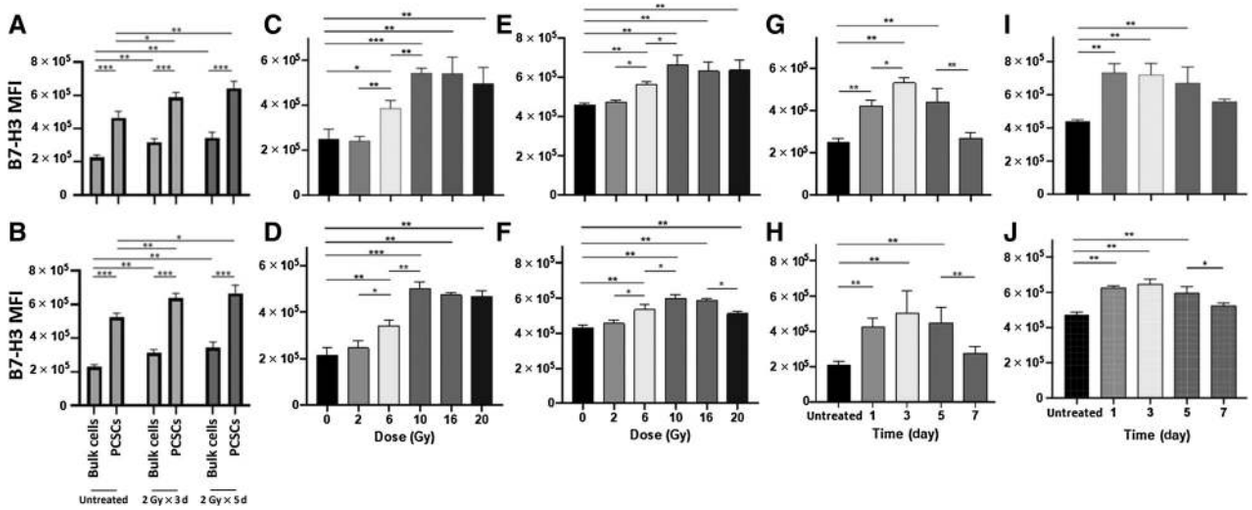

Figure 4.

FIR or IR upregulates B7-H3 expression on PCSCs and bulk prostate cancer cells. Sorted ALDH$^+$CD44$^+$ PCSCs and unsorted bulk tumor cells were treated with FIR at doses and times indicated and 24 hours later, the irradiated and nonirradiated (untreated) cells were stained for B7-H3 cell surface expression with B7-H3-specific mAb 376.96. Flow cytometry analysis of B7-H3$^+$ bulk tumor cells and PCSCs under each indicated treatment condition were performed. Histograms of flow analysis are shown in Supplementary Fig. S1 and mean ± SD of B7-H3 MFI are shown for DU145 (**A**) and PC3 cells (**B**). A single variable dose of IR (0–20 Gy) was given to prostate cancer bulk cells or PCSCs and 24 hours later, B7-H3 expression was detected by flow cytometry analysis. Histograms of flow analysis are shown in Supplementary Fig. S2 and mean ± SD of B7-H3 MFI for DU145 bulk cells (**C**) and PCSCs (**E**) and PC3 bulk cells (**D**) and PCSCs (**F**) are shown. A single dose of IR (10 Gy) was given to prostate cancer bulk cells or PCSCs, B7-H3 expression was detected at the indicated time points. The histograms of flow analysis are shown in Supplementary Fig. S2 and mean ± SD of B7-H3 MFI for DU145 bulk cells (**G**) and PCSCs (**I**) and PC3 bulk cells (**H**) and PCSCs (**J**) are shown. The experiments were repeated three times (*, $P < 0.05$; **, $P < 0.01$; ***, $P < 0.001$).

PCSCs express higher levels of B7-H3 antigen than bulk prostate cancer cells

In general, CAR T-cell therapy is antigen-specific, and its efficacy is dependent on the level of expression of the targeted antigen on the tumor cell (17). Recently, we developed an effective therapeutic strategy for PDAC using CAR T cells that target B7-H3 (15). As the first step in applying this strategy to prostate cancer, the level of B7-H3 expression on PCSCs in the prostate cancer cell lines was studied. Although 100% of PCSCs and bulk tumor populations expressed B7-H3, its expression on PCSCs was found to be significantly higher in both cell lines, as measured by mean fluorescence intensity [MFI; 2.4-fold higher in DU145 cells ($P < 0.001$) and 2.2-fold higher in PC3 cells ($P < 0.001$); **Fig. 3A–D**]. The flow data are specific, as SUM159 B7-H3 KO cells, and Raji cells, which do not express endogenous B7-H3 served as controls and stained negative (**Fig. 3E** and **F**).

FIR enhances B7-H3 expression on PCSCs and bulk prostate cancer cells

For a rational basis in designing a combinational approach using FIR and B7-H3 CAR T cells to treat prostate cancer, the impact of FIR on B7-H3 expression by PCSCs and bulk prostate cancer cell populations in DU145 and PC3 cells was investigated by flow analysis with B7-H3-specific mAb 376.96 (Supplementary Fig. S1A and B). In both prostate cancer cell lines tested, FIR (both doses) significantly increased B7-H3 expression levels on PCSCs and bulk prostate cancer cell populations compared with untreated cells, as determined by MFI ($P < 0.05$). The total FIR dose, however, did not seem to make a significant difference on B7-H3 expression by either cell population. Moreover, regardless of treatment, PCSCs expressed significantly more B7-H3 than bulk cells ($P < 0.001$; **Fig. 4A** and **B**). In addition, a single dose of IR increased B7-H3 expression on both PCSCs and bulk cells in a dose-dependent manner up to 10 Gy, with significant B7-H3 upregulation observed at 6 Gy ($P < 0.05$), 10 Gy ($P < 0.01$), 16 Gy ($P < 0.01$), and 20 Gy ($P < 0.01$). However, a single dose of >10 Gy IR (16 or 20 Gy) did not further increase B7-H3 expression on either bulk cells (**Fig. 4C**, **D**) or PCSCs (**Fig. 4E** and **F**; Supplementary Fig. S2A and S2B). 10 Gy single dose IR-induced B7-H3 upregulation on bulk cells was also time-dependent, with B7-H3 expression greater on day 3 versus day 1 post-IR ($P < 0.05$) in DU145 cells and a trend toward this in PC3 cells. However, B7-H3 expression started to drop by day 5 post-IR and by day 7, the levels of B7-H3 were not significantly different from untreated cells ($P > 0.05$; **Fig. 4G**, **H**). In contrast, 10 Gy single dose IR-induced B7-H3 upregulation on PCSCs lasted from days 1 to 5 post-IR without much change. By day 7 post-IR, the levels of B7-H3 were not significantly different from untreated cells ($P > 0.05$; **Fig. 4I** and **J**; Supplementary Fig. S2C and S2D).

Generation and phenotype of B7-H3 CAR T cells

To generate B7-H3 CAR T cells for use in therapy of cancer, the mAb 376.96 scFv used to determine B7-H3 expression by prostate cancer was selected as the CAR of the retroviral construct. It was linked with a CD8α hinge and transmembrane domain, followed by a CD28 costimulatory domain coupled to a CD3ζ intracellular signaling domain (**Fig. 5A**) (15). PBMCs isolated from three healthy donors were cultured in the presence or absence of retroviral construct supernatants and used to generate B7-H3 CAR T cells and NT cells, respectively. Both populations expanded equally over time (**Fig. 5B**). After 8 days of culture, 64 ± 4.36% of the transduced CAR T cells derived from PBMCs obtained from the three donors were positive, whereas NT cells were negative for surface expression of the B7-H3-specific scFv 376.96 by flow cytometry (**Fig. 5C**). After 11 days of culture, the number of B7-H3 CAR T cells and NT cells both increased more than 10-fold

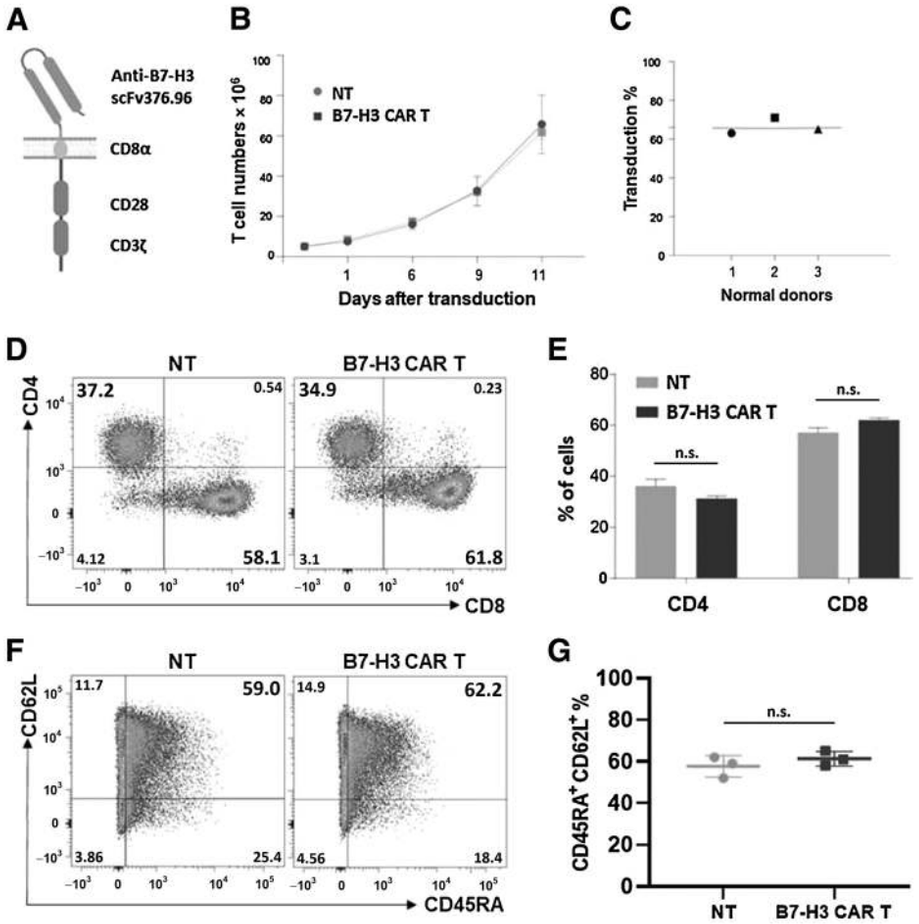

Figure 5.

Generation and phenotype of B7-H3 CAR T cells. Illustration of the B7-H3 CAR construct consisting of anti-human B7-H3 scFv 376.96, CD28 costimulatory domain, and CD3ζ signaling domain (**A**). The time course for the expansion of transduced CAR T and NT cells (**B**), as well as the percentages of B7-H3 CAR T cells out of the total $CD3^+$ cells on day 8 in transduced T cells expanded from three individual donors are shown (**C**). Flow cytometry analysis of B7-H3 CAR T cells and NT cells for $CD4^+$ and $CD8^+$ T cells (**D**) and mean ± SD (%) of $CD4^+$ and $CD8^+$ CAR T cells are shown (**E**), in addition, flow cytometry analysis for $CD45RA^+CD62L^+$ memory-CAR T cells (**F**) and mean ± SD (%) $CD45RA^+CD62L^+$ CAR T cells (**G**) are shown. n.s., not significant.

(**Fig. 5B**), but NT cells continued to show nondetectable levels of 376.96 scFv expression. The B7-H3 CAR T cells and NT cells showed a similar percentage of $CD4^+$ (35.42 ± 2.08% vs. 37.73 ± 0.74%; $P = 0.1342$) and $CD8^+$ T cells (62.67 ± 1.21% vs. 58.26 ± 0.35%; $P = 0.2495$); as well as a similar percentage of memory $CD45RA^+CD62L^+$ T cells (61.33 ± 3.51% vs. 57.67 ± 5.13%; $P = 0.3648$; **Fig. 5D–G**).

PCSCs are more sensitive to B7-H3 CAR T cells than bulk prostate cancer cells *in vitro*

To assess whether the B7-H3 CAR T cells were able to mediate cytolysis of PCSCs, sorted $ALDH^+CD44^+$ PCSCs cells and bulk prostate cancer cells were co-cultured with B7-H3 CAR T cells at different E:T ratios for 48 hours. As measured by MTT assays, cytolysis of both cell populations by B7-H3 CAR T cells in each cell line tested was dose- and antigen expression level-dependent. At E:T ratio of 5:1, >95% of PCSCs and bulk prostate cancer cells were killed, whereas at E:T ratio of 1:1, 63.41 ± 3.32% PCSCs and 30.82 ± 4.67% bulk cells of the DU145 cell line ($P < 0.001$), as well as 66.90 ± 0.19% PCSCs and 30.22 ± 3.40% bulk cells of the PC3 cell line ($P < 0.001$) were eliminated. In contrast, at E:T ratio of 1:5, there was almost no killing of either target cell population. Importantly, analysis of the two whole curves (all three E:T: ratios) confirmed that B7-H3 CAR T cell-mediated cytotoxicity is greater on PCSCs than on bulk cells in cell lines DU145 ($P < 0.001$) and PC3 ($P < 0.001$; **Fig. 6A** and **B**). The cytolysis was antigen-specific, as use of NT effectors or SUM159 B7-H3 KO cells as targets resulted in no measurable cytotoxicity (**Fig. 6C**). In addition, cytotoxicity of B7-H3 CAR T cells against sorted PCSCs irradiated at 2 Gy/day x 5 days was tested by flow analysis. At E:T ratio of 1:1, PCSCs were almost nondetectable (**Fig. 6D**). This observation was confirmed by the results of the sphere formation assay. Co-culturing FIR-treated PCSCs with B7-H3 CAR T cells (E:T ratio of 1:1) reduced the sphere forming ability 16- and 20-fold for DU145 ($P < 0.001$) and PC3 ($P < 0.001$) cell lines, respectively, compared with FIR-treated PCSCs co-cultured with NT cells (**Fig. 6E** and **F**).

Targeting FIR-resistant PCSCs with B7-H3 CAR T cells is more effective than either FIR or CAR T cells alone in inhibiting growth of hormone-insensitive prostate cancer xenografts in immunodeficient mice

The demonstrated ability of B7-H3 CAR T cells to eliminate FIR-resistant PCSCs and bulk prostate cancer cells *in vitro* (**Fig. 6**) provided a strong rationale to test if this strategy would be effective in a preclinical prostate cancer xenograft tumor model system using immunodeficient mice bearing DU145 cell line–derived xenografts. The DU145 cell line was derived from a brain metastatic prostate tumor and is hormone insensitive (40), representative of a highly clinically relevant type of prostate cancer (castration-resistant prostate cancer) that is associated with very poor clinical outcomes. FIR was administered over a 5-day period (days 11–15) post-tumor cell inoculation (day 0). B7-H3 CAR T cells were administered on day 15 (**Fig. 7A**), with tumor volumes being monitored biweekly up until

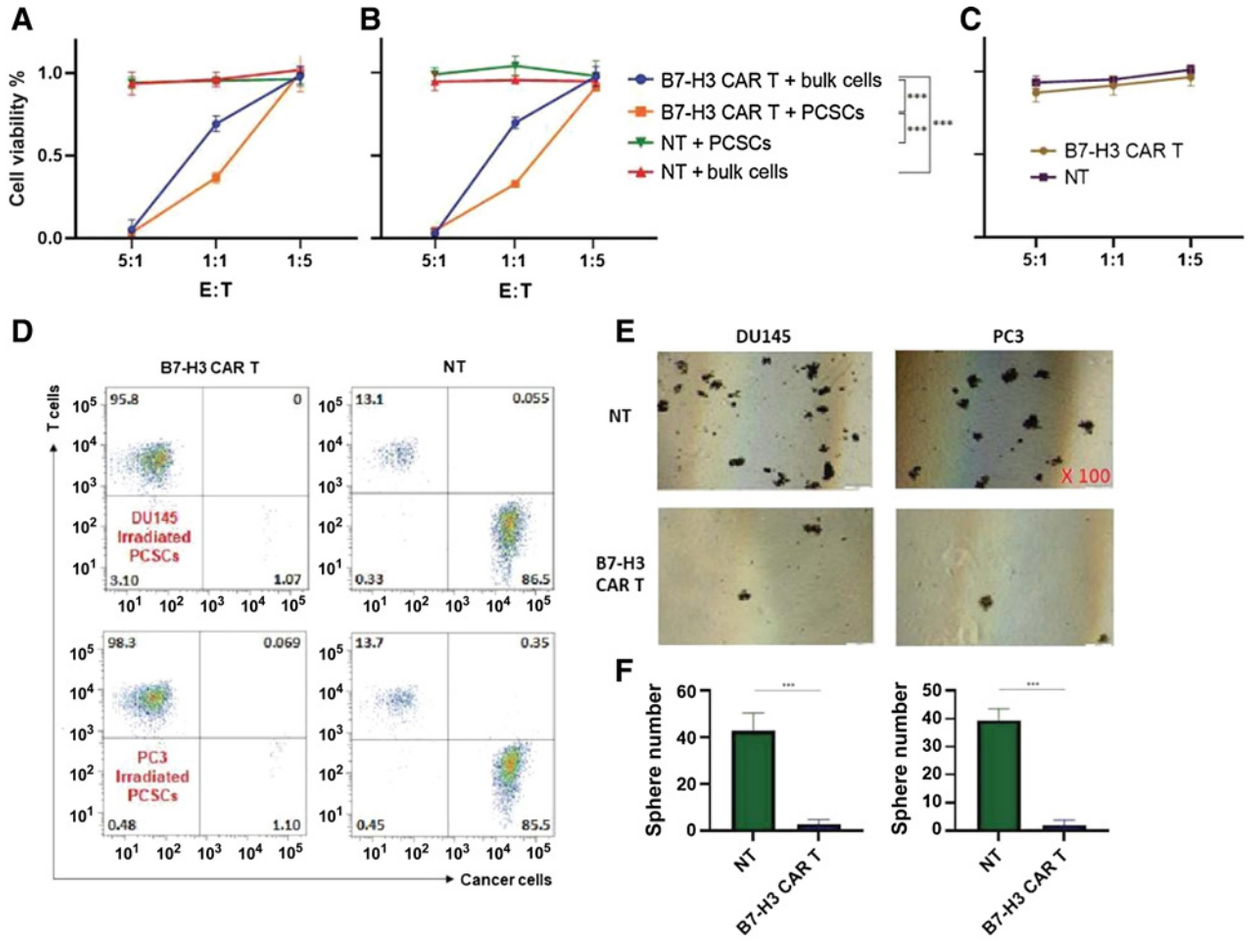

Figure 6.

PCSCs are more sensitive to B7-H3 CAR T cells than bulk prostate cancer cells *in vitro*. B7-H3 CAR T cells and sorted ALDH$^+$CD44$^+$ PCSCs or unsorted bulk prostate cancer target cells were co-cultured at indicated E:T ratios for 48 hours. CAR T cells in the cell suspension were removed, and the viability of adherent target cells was quantitated by MTT assays. The viability of different cell populations in the cell line DU145 (**A**), PC3 (**B**), and SUM159 B7-H3 KO cells (**C**) are shown. Separately, FIR treated ALDH$^+$CD44$^+$ PCSCs target cells were co-cultured with B7-H3 CAR T cells at E:T ratio of 1:1 for 48 hours. The co-cultured cells were analyzed for CD3$^+$ CAR T cells (T cells) and B7-H3$^+$ residual PCSCs (cancer cells; **D**). NT or B7-H3 CAR T cells were co-cultured with FIR treated PCSCs at E:T ratio of 1:1 for 24 hours. Then, the cells were trypan blue stained to exclude dead cells, and living cells were tested for their ability to form spheres. After 7 to 10 days, small spheres were detected by microscopy. At day 18, spheres/well were counted and photographed (100 ×; **E**). Mean ± SD of spheres/well for DU145 (**F**, left) and PC3 (**F**, right) are shown. NT cells were used as negative controls in these experiments. FIR dosage used was 2 Gy/day for 5 days. The experiments were repeated three times (***, $P < 0.001$).

day 60. The antitumor efficacy (as monitored by tumor volume) of the combination of B7-H3 CAR T cells with FIR was significantly greater than either FIR ($P < 0.001$) or B7-H3 CAR T cells alone ($P < 0.001$; **Fig. 7B** and **H**). No treatment-associated toxicity was detected as measured by mouse general health conditions and body weight (**Fig. 7C**). As anticipated, the greater antitumor efficacy of B7-H3 CAR T cells and FIR was associated with a decreased percentage of PCSCs in tumors (0.045 ± 0.021%), identified as ALDH$^+$CD44$^+$ cells, compared with untreated tumors (0.76 ± 0.12%, $P < 0.05$) and tumors treated with FIR+NT cells (1.35 ± 0.13%, $P < 0.01$), as assessed by flow analysis (**Fig. 7D** and **E**). Although the difference was not significant compared with tumors treated with B7-H3 CAR T cells alone (0.22 ± 0.14%, $P = 0.2257$)(**E**), when PCSCs were defined as sphere forming cells, from samples of tumors treated by B7-H3 CAR T cells and FIR displayed a significantly lower number of PCSCs (2.4 ± 0.89) compared with untreated tumors (20.2 ± 1.3, $P < 0.001$), tumors treated with FIR+NT alone (49.2 ± 5.63, $P < 0.001$), and tumors treated with B7-H3 CAR T cells alone (10.4 ± 1.14, $P < 0.001$; **Fig. 7F** and **G**). It is noteworthy that these *in vivo* data indicate FIR increased PCSCs; this conclusion is in agreement with previous *in vitro* findings of FIR inducing PCSCs (**Fig. 1**). To confirm these data and identify the optimal timing for the combination of FIR and B7-H3 CAR T cells, we tested FIR combined with B7-H3 CAR T cells given at different days post-FIR in immunodeficient NSG mice bearing xenografts derived from PC3, the other castration-resistant prostate cancer cell line used in this study (**Fig. 8A**). We found that the combination of FIR and B7-H3 CAR T cells is more effective than FIR alone at inhibiting growth (as monitored by tumor volume) of hormone-insensitive PC3 xenografts regardless of whether B7-H3 CAR T cells were given 1, 3, or 7 days post-FIR ($P < 0.001$; **Fig. 8B**). However, the antitumor effect of the combination was the greatest 3 days post-FIR [FIR(3)+B7-H3 CAR T vs. FIR(1)+B7-H3 CAR T: $P < 0.01$; FIR(3)+B7-H3 CAR T vs.

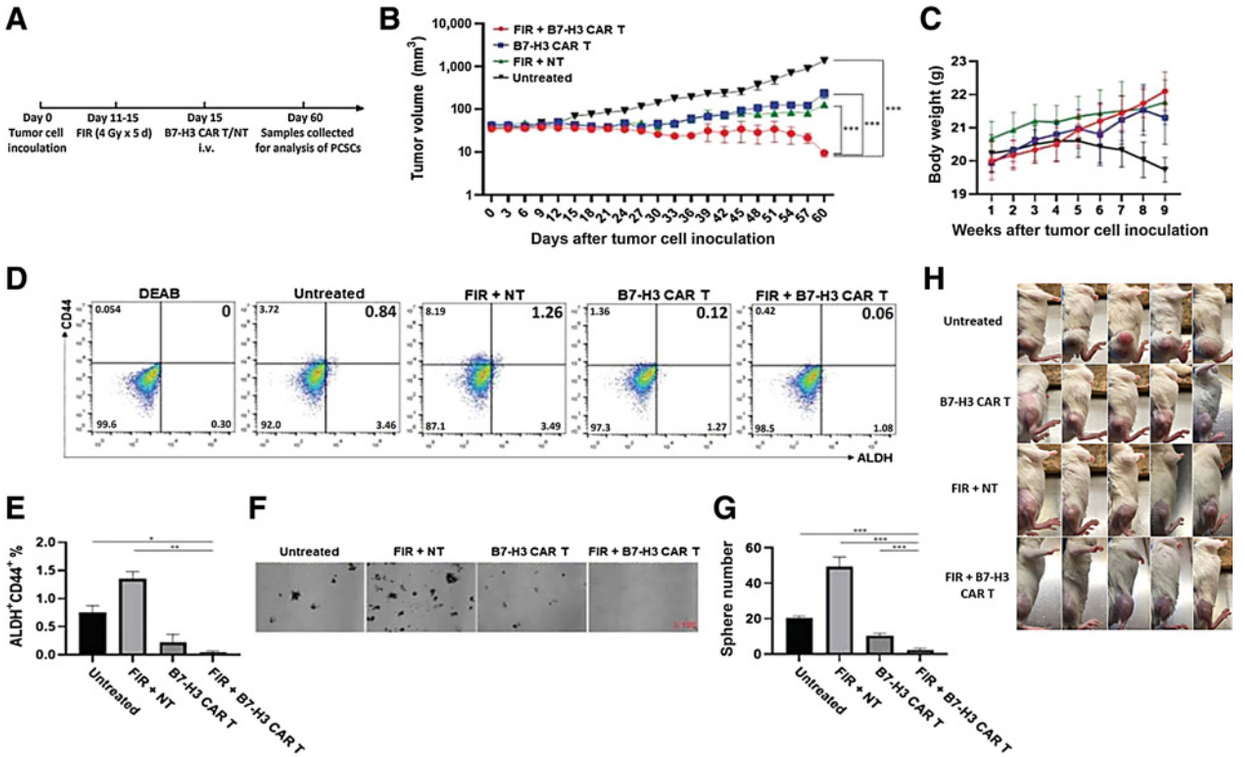

Figure 7.

FIR and B7-H3 CAR T-cell combinatorial therapy is more effective than either FIR or B7-H3 CAR T cells alone in inhibiting growth of a hormone-insensitive DU145 prostate cancer xenograft model. Schematic diagram of the experimental schedule (**A**), mean ± SEM of tumor volume (**B**), and body weight (**C**) are shown. At the time of sacrifice, the tumor from each mouse was collected. A single cell suspension from two pooled tissue samples (tumors from 5 mice of the same group were pooled into two pools: one pool consists of two and the other pool consists of three tissue samples) from each group was assessed by flow cytometry for $ALDH^+CD44^+$ PCSCs (**D**) and mean ± SD (%) of $ALDH^+CD44^+$ PCSCs are shown (**E**). Pools were also analyzed for sphere formation. Shown are representative photographs (×100; **F**) and mean ± SD of spheres/well (**G**). Photos of tumor-bearing mice are also shown (**H**; *, $P < 0.05$; **, $P < 0.01$; ***, $P < 0.001$).

FIR(7)+B7-H3 CAR T: $P < 0.001$]. Moreover, CAR T-cell administration 1 day post-FIR was more effective than administration 7 days post-FIR [FIR(1)+B7-H3 CAR T vs. FIR(7)+B7-H3 CAR T: $P < 0.001$; **Fig. 8B**]. These data indicate that the duration of FIR-induced B7-H3 upregulation (1–3 days post-FIR; Supplementary Fig. S3A and S3C) is associated with the optimal time-window of B7-H3 CAR T-cell administration post-FIR for the greatest antitumor efficacy (**Fig. 8B**). Once again, the antitumor efficacy of the combination of FIR and B7-H3 CAR T cells was inversely associated with the number of PCSCs within tumors, measured either as $ALDH^+CD44^+$ cells (**Fig 8D** and **E**) or sphere forming cells (**Fig. 8F** and **G**).

Discussion

Although RT (FIR) is an important therapy for newly diagnosed localized prostate cancer and/or low-volume metastatic prostate cancer, the resistance of PCSCs to radiation can hinder achieving beneficial therapeutic outcomes in many cases (12, 36). Therefore, it is critical to develop an effective therapeutic approach to enhance radiation in eradicating PCSCs, the subpopulation of tumor cells that have been shown to be highly resistant to chemotherapy and radiation in many types of human malignancies. PCSCs like other CSCs are considered to be a major cause of treatment failure that ultimately results in recurrence and metastasis (10, 12).

The preclinical findings reported here establish the immune checkpoint B7-H3 as an attractive candidate for CAR T-cell–based immunotherapy of prostate cancer that is resistant to FIR. The ability to target the immune checkpoint B7-H3 expressed on human PCSCs and bulk prostate cancer cells using B7-H3 CAR T cells was established in a series of experiments. We first demonstrated extensive and higher levels of B7-H3 expression on PCSCs compared with bulk prostate cancer cells using the B7-H3-specfic mAb 376.96 (**Fig. 3**), which was made in our laboratory. scFv 376.96 was used for generation of the B7-H3 CAR T-cell construct. Subsequent experiments established the efficient and specific ability of B7-H3 CAR T cells to target $B7\text{-}H3^+$ PCSCs and bulk prostate cancer cells and mediate cytolysis of $B7\text{-}H3^+$ cells in *in vitro*-based assays. The cytotoxic activity of the CAR T cells was high. All nonirradiated $B7\text{-}H3^+$ target cells tested were eliminated at an E:T ratio of 5:1. When tested at a lower E:T ratio, the cytotoxicity of B7-H3 CAR T cells was found to be higher against PCSCs than against bulk prostate cancer cells; the former express higher levels of B7-H3 compared with bulk cells (**Fig. 6**). Most importantly, FIR upregulated B7-H3 expression on PCSCs and bulk prostate cancer cells in both cell lines tested. Enhanced B7-H3 expression by PCSCs was IR dose- and time-dependent (**Fig. 4**). Furthermore, B7-H3 CAR T cells were found to be able to effectively eliminate FIR-resistant PCSCs *in vitro* (E:T ratio of 1:1) and *in vivo* (a single injection of 2×10^6 cells; **Figs. 6–8**). As a result, the combination of FIR (4 Gy/day × 5 days) and B7-H3 CAR T cells was more effective in controlling both

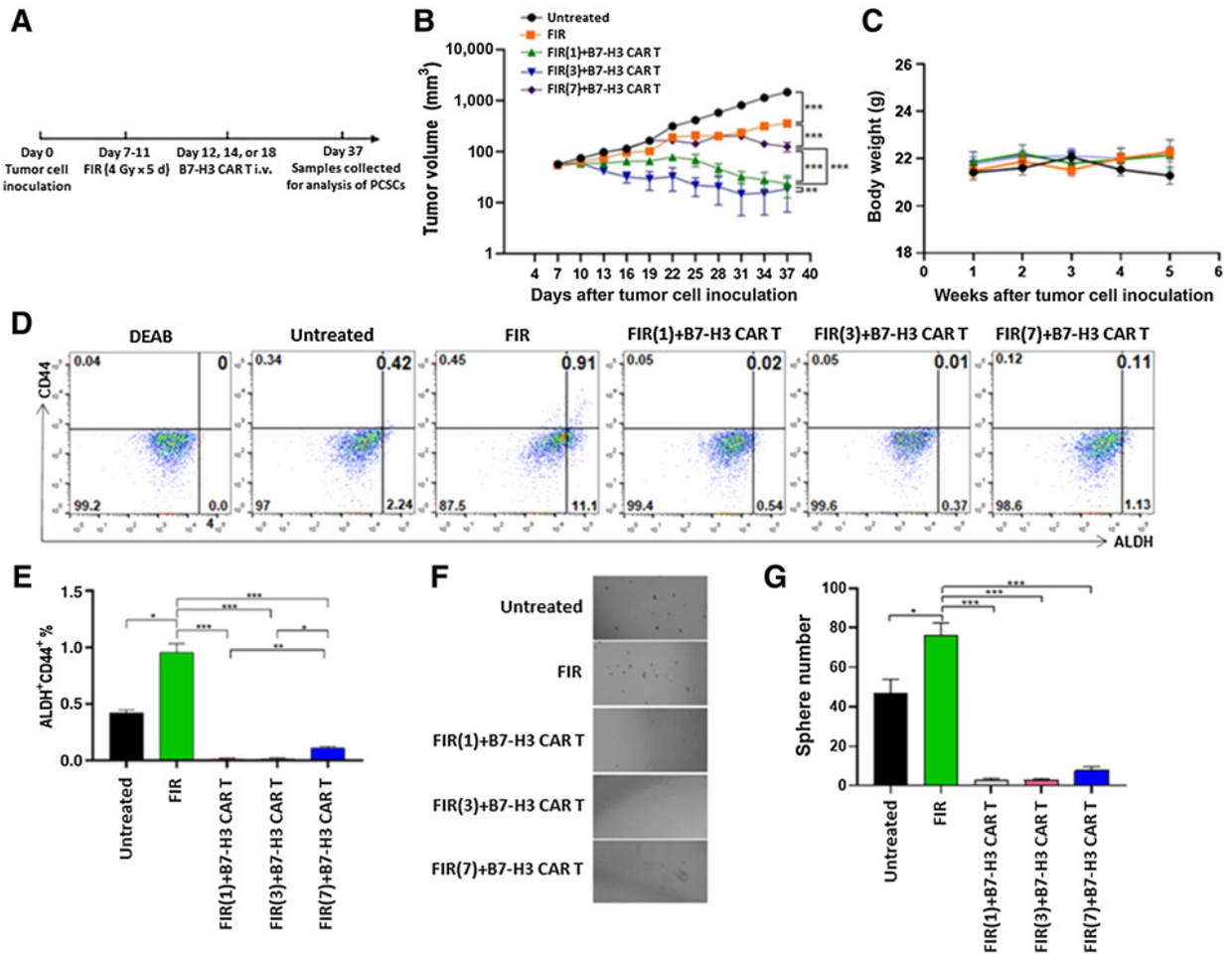

Figure 8.

Efficacy of FIR and B7-H3 CAR T-cell combinatorial therapy in inhibiting growth of a hormone-insensitive PC3 prostate cancer xenograft model is optimal when B7-H3 CAR T cells are administered 1 to 3 days post-FIR. Schematic diagram of the experimental schedule (**A**), mean ± SEM of tumor volume (**B**), and body weight (**C**) are shown. At the time of sacrifice, the tumor from each mouse was collected. A single cell suspension from two pooled tissue samples (tumors from 5 mice of the same group were pooled into two pools: one pool consists of two and the other pool consists of three tissue samples) from each group was assessed by flow cytometry for $ALDH^+CD44^+$ PCSCs (**D**) and mean ± SD (%) of $ALDH^+CD44^+$ PCSCs are shown (**E**). Pools were also analyzed for sphere formation. Shown are representative photographs (×100; **F**) and mean ± SD of spheres/well (**G**; *, $P < 0.05$; **, $P < 0.01$; ***, $P < 0.001$).

DU145- and PC3-derived prostate cancer xenograft growth in NSG mice than FIR or B7-H3 CAR T cells administered as monotherapies (**Fig. 7**, **8**). It is noteworthy that the duration of FIR or single-dose irradiation (IR)-induced upregulation of B7-H3 on prostate cancer cells and PCSCs lasts for up to 3 days (**Fig. 4G–J**; Supplementary Fig. S3A and S3C), which is associated with the optimal time-window for B7-H3 CAR T *in vivo* delivery, that is, 1 to 3 days post-FIR (although 3 days appeared to be slightly better than 1 day), to achieve its greatest antitumor efficacy in the PC3-derived xenograft mouse model (**Fig. 8**).

To our knowledge, this is the first study to demonstrate the potential of targeting the immune checkpoint B7-H3, which is highly expressed on FIR-resistant PCSCs, with a CAR T-cell therapy to achieve beneficial outcomes for prostate cancer. The study by Deng and colleagues, aimed at targeting PCSCs expressing EPCaM by EPCaM-specific CAR T cells in xenograft PC3 prostate cancer models, had only modest antitumor efficacy compared with treatment with NT cells (41). Combinatorial approaches to cancer treatment involving systemic therapy and RT protocols may be more effective than monotherapies. Attempts have been made to use RT to increase efficacy of CAR T-cell therapy for cancer in preclinical and clinical studies. The combination of a single dose of IR (4 Gy) with NKG2D CAR T cells in one study and IR (2 Gy) with sLeA CAR T cells in another was shown to enhance the cytotoxicity against tumor cells *in vitro* and in murine glioblastoma cells orthotopically grafted in syngeneic immunocompetent mice and in human PDAC cells orthotopically grafted in immunodeficient mice, respectively (42, 43). In the glioblastoma study, the mechanisms of synergy between IR and CAR T cells were attributed to increased IFNγ production by tumor-infiltrating CAR T cells and their accumulation within the tumor microenvironment (42), whereas enhanced sensitivity of the IR-treated PDAC cells to apoptosis appeared to be mediated by TRAIL produced by the tumor-engaged sLeA CAR T cells (43). More importantly, another clinical trial showed that patients with diffuse large B-cell lymphoma given RT (40 Gy in 2 Gy/fraction) to debulk tumor burden before infusion of CAR T cells against CD19,

CD20, or CD22, had better clinical responses but also experienced only mild cytokine release syndrome (CRS; grade 1/2) and no neurotoxicity, which are the typical adverse events associated with CAR T therapy, compared with the cohort treated with intensive combined chemotherapy to debulk tumor burden. All the patients in the latter group experienced CAR T-cell-related severe CRS (grade 3/4/5) and 75% of patients experienced neurotoxicity (44). Consistent with these findings are the results of a clinical trial in patients with relapsed or refractory aggressive B-cell lymphoma who received bridging-RT within 30 days of CAR T cell infusion (median bridging-RT dose was 37.5 Gy and was completed a median of 13 days before infusion of CAR T cells against CD19) and who did not experience serious CRS or neurotoxicity (45).

In agreement with these preclinical and clinical reports, the results of this study not only provide evidence to support B7-H3 CAR T therapy and the need to combine it with RT in prostate cancer, but also offer potential additional advantages as follows (i) establish B7-H3 as an important target for prostate cancer on both PCSCs and bulk prostate cancer cells, (ii) may provide an opportunity to enhance activity of CAR T cells and tumor-infiltrating CTLs by targeting immune checkpoint B7-H3 using CAR T cells, and (iii) IR could potentiate the effects of CAR T cells by providing a favorable tumor microenvironment and increased density of infiltrating CTLs by upregulation of MHC class I (46, 47). Thus, the approach presented in this paper provides a sound basis for further development of this unique combinatorial model of RT and B7-H3 CAR T-cell therapy for prostate cancer in a complementary manner for better clinical outcomes.

It is noteworthy that accumulated data from dose escalation studies in the past decades have suggested that high-dose IR may improve biochemical-failure survival and/or metastasis-free survival, but dose escalation is limited by presence of adjacent normal tissues/organs and is often associated with increased risks for normal tissue toxicities in patients with prostate cancer (48, 49). Clearly, results of this study suggest that combination of B7-H3 CAR T cells with RT should be investigated to improve clinical outcomes in localized prostate cancer with high-risk features and/or low-volume metastasis. In addition, it is known that CAR T-cell infusion before IR in the clinical setting worked well (44, 45). A case study of a refractory myeloma patient in which FIR (20 Gy in 4 Gy/fraction) was delivered locally, shortly after BCMA-targeted CAR T-cell therapy showed a potential synergistic clinical response and T-cell clonal expansion (50). Therefore, the sequence of CAR T-cell administration in relation to RT, for example, either before, during or after RT, should be further compared and optimized. Likewise, the dose and frequency of RT in combination with a given CAR T-cell therapy must also be tested and optimized in the future to maximize therapeutic ratio, improving efficacy while minimizing toxicity for patients with prostate cancer.

Authors' Disclosures

G. Dotti reports grants from Cell Medica, Bellicum Pharmaceutical, and Bluebird Bio, personal fees from Bellicum Pharmaceutical, Molmed s.p.a., and Catamaran, and other from Bluebird Bio outside the submitted work; and also has a patent for Patent on the B7-H3.CAR issued and licensed to Bluebird Bio. S. Ferrone and X. Wang report a patent on the B7-H3.CAR issued and licensed to Bluebird Bio. No disclosures were reported by the other authors.

Authors' Contributions

Y. Zhang: Conceptualization, formal analysis, funding acquisition, investigation, writing–original draft, writing–review and editing. **L. He:** Formal analysis, investigation. **A. Sadagopan:** Formal analysis, investigation, writing–review and editing. **T. Ma:** Formal analysis, investigation. **G. Dotti:** Formal analysis, investigation, writing–review and editing. **Y. Wang:** Formal analysis, investigation. **H. Zheng:** Formal analysis, writing–review and editing. **X. Gao:** Formal analysis, writing–review and editing. **D. Wang:** Formal analysis, writing–review and editing. **A.B. DeLeo:** Formal analysis, writing–review and editing. **S. Fan:** Formal analysis, investigation. **R. Sun:** Formal analysis, investigation. **L. Yu:** Formal analysis, investigation. **L. Zhang:** Formal analysis, investigation. **G. Wang:** Formal analysis, writing–review and editing. **S. Ferrone:** Funding acquisition, writing–review and editing. **X. Wang:** Conceptualization, resources, formal analysis, supervision, funding acquisition, methodology, writing–original draft, project administration, writing–review and editing.

Acknowledgments

This work was supported by grants R01CA226981-01A1 (to X. Wang), W81XWH-16-1-0500 Department of Defense Breakthrough Award Level 2 (to S. Ferrone), R03CA223886 (to S. Ferrone), R01DE028172 (to S. Ferrone), R03CA231766 (to S. Ferrone), W81XWH-20-1-0315 (BC190615) Department of Defense grant (to S. Ferrone), and Natural Science Foundation of Jiangxi Province 20202BAB206018 (to Y. Zhang).

The costs of publication of this article were defrayed in part by the payment of page charges. This article must therefore be hereby marked *advertisement* in accordance with 18 U.S.C. Section 1734 solely to indicate this fact.

Received May 29, 2020; revised November 13, 2020; accepted January 4, 2021; published first March 2, 2021.

References

1. American Cancer Society. Cancer facts & figures 2020. Available from: https://www.cancer.org/research/cancer-facts-statistics/all-cancer-facts-figures/cancer-facts-figures-2020.html.
2. Punnen S, Cooperberg MR, D'Amico AV, Karakiewicz PI, Moul JW, Scher HI, et al. Management of biochemical recurrence after primary treatment of prostate cancer: a systematic review of the literature. Eur Urol 2013;64:905–15.
3. NCCN. NCCN Clinical Practice Guidelines in Oncology (NCCN Guidelines) Prostate Cancer Version 1.2020. Available from: https://www.nccn.org/professionals/physician_gls/default.aspx.
4. Rosenbaum E, Partin A, Eisenberger MA. Biochemical relapse after primary treatment for prostate cancer: studies on natural history and therapeutic considerations. J Natl Compr Canc Netw 2004;2:249–56.
5. Simmons MN, Stephenson AJ, Klein EA. Natural history of biochemical recurrence after radical prostatectomy: risk assessment for secondary therapy. Eur Urol 2007;51:1175–84.
6. Chaiswing L, Weiss HL, Jayswal RD, Clair DKS, Kyprianou N. Profiles of radioresistance mechanisms in prostate cancer. Crit Rev Oncog 2018;23:39–67.
7. Morgan PB, Hanlon AL, Horwitz EM, Buyyounouski MK, Uzzo RG, Pollack A. Timing of biochemical failure and distant metastatic disease for low, intermediate, and high risk prostate cancer after radiotherapy. Cancer 2007;110:68–80.
8. Cong J, Wang Y, Zhang X, Zhang N, Liu L, Soukup K, et al. A novel chemoradiation targeting stem and nonstem pancreatic cancer cells by repurposing disulfiram. Cancer Lett 2017;409:9–19.
9. Wang Y, Li W, Patel SS, Cong J, Zhang N, Sabbatino F, et al. Blocking the formation of radiation–induced breast cancer stem cells. Oncotarget 2014;5:3743.
10. Mei W, Lin X, Kapoor A, Gu Y, Zhao K, Tang D. The contributions of prostate cancer stem cells in prostate cancer initiation and metastasis. Cancers 2019;11:434.
11. Ni J, Cozzi P, Hao J, Duan W, Graham P, Kearsley J, et al. Cancer stem cells in prostate cancer chemoresistance. Curr Cancer Drug Targets 2014;14:225–40.
12. Tsing T, Beretov J, Ni J, Bai X, Bucci J, Graham P, et al. Cancer stem cells in prostate cancer radioresistance. Cancer Lett 2019;465:94–104.
13. Kantoff PW, Higano CS, Shore ND, Berger ER, Small EJ, Penson DF, et al. Sipuleucel-T immunotherapy for castration-resistant prostate cancer. N Engl J Med 2010;363:411–22.
14. Boettcher AN, Usman A, Morgans AK, VanderWeele D, Sosman J, Wu J. Past, current, and future of immunotherapies for prostate cancer. Front Oncol 2019;9:884.

15. Du H, Hirabayashi K, Ahn S, Kren NP, Montgomery SA, Wang X, et al. Antitumor responses in the absence of toxicity in solid tumors by targeting B7-H3 via chimeric antigen receptor T cells. Cancer Cell 2019;35:221–37.
16. June CH, O'Connor RS, Kawalekar OU, Ghassemi S, Milone MC. CAR T cell immunotherapy for human cancer. Science 2018;359:1361–65.
17. Majzner RG, Mackall CL. Tumor antigen escape from CAR T-cell therapy. Cancer Discov 2018;8:1219–26.
18. Shah N, Maatman T, Hari PN, Johnson B. Multi targeted CAR-T cell therapies for B-cell malignancies. Front Oncol 2019;9:146.
19. Gorchakov AA, Kulemzin SV, Kochneva GV, Taranin AV. Challenges and prospects of chimeric antigen receptor T-cell therapy for metastatic prostate cancer. Eur Urol 2020;77:299–308.
20. Heinrich M-C, Göbel C, Kluth M, Bernreuther C, Sauer C, Schroeder C, et al. PSCA expression is associated with favorable tumor features and reduced PSA recurrence in operated prostate cancer. BMC Cancer 2018;18:612.
21. Trover JK, Beckett ML, Wright GL Jr. Detection and characterization of the prostate specific membrane antigen (PSMA) in tissue extracts and body fluids. Int J Cancer 1995;62:552–58.
22. Zappasodi R, Merghoub T, Wolchok JD. Emerging concepts for immune checkpoint blockade-based combination therapies. Cancer Cell 2018;33:581–98.
23. Benzon B, Zhao S, Haffner M, Takhar M, Erho N, Yousefi K, et al. Correlation of B7-H3 with androgen receptor, immune pathways and poor outcome in prostate cancer: an expression-based analysis. Prostate Cancer Prostatic Dis 2017;20: 28–35.
24. Chavin G, Sheinin Y, Crispen PL, Boorjian SA, Roth TJ, Rangel L, et al. Expression of immunosuppresive B7-H3 ligand by hormone-treated prostate cancer tumors and metastases. Clin Cancer Res 2009;15:2174–80.
25. Powderly J, Cote G, Flaherty K, Szmulewitz R, Ribas A, Weber J. Interim results of an ongoing phase 1, dose escalation study of MGA271 (Enoblituzumab), an Fc-optimized humanized anti-B7-H3 monoclonal antibody, in patients with advanced solid cancer. J Immuno Ther Cancer 2015;3:8.
26. Kontos F, Michelakos T, Kurokawa T, Sadagopan A, Schwab JH, Ferrone CR, et al. B7-H3: an attractive target for antibody-based immunotherapy. Clin Cancer Res 2020.
27. Suh W-K, Gajewska BU, Okada H, Gronski MA, Bertram EM, Dawicki W, et al. The B7 family member B7-H3 preferentially down-regulates T helper type 1–mediated immune responses. Nat Immunol 2003;4:899–906.
28. Ma J, Ma P, Zhao C, Xue X, Han H, Liu C, et al. B7-H3 as a promising target for cytotoxicity T cell in human cancer therapy. Oncotarget 2016;7:29480.
29. Fizazi K, Tran N, Fein L, Matsubara N, Rodriguez-Antolin A, Alekseev BY, et al. Abiraterone plus prednisone in metastatic, castration-sensitive prostate cancer. N Engl J Med 2017;377:352–60.
30. Parker CC, James ND, Brawley CD, Clarke NW, Hoyle AP, Ali A, et al. Radiotherapy to the primary tumour for newly diagnosed, metastatic prostate cancer (STAMPEDE): a randomised controlled phase 3 trial. Lancet North Am Ed 2018;392:2353–66.
31. Sweeney CJ, Chen Y-H, Carducci M, Liu G, Jarrard DF, Eisenberger M, et al. Chemohormonal therapy in metastatic hormone-sensitive prostate cancer. N Engl J Med 2015;373:737–46.
32. Sun T, Yang W, Toprani SM, Guo W, He L, DeLeo AB, et al. Induction of immunogenic cell death in radiation-resistant breast cancer stem cells by repurposing anti-alcoholism drug disulfiram. Cell Commun Signal 2020;18: 1–14.
33. Kasten BB, Gangrade A, Kim H, Fan J, Ferrone S, Ferrone CR, et al. 212Pb-labeled B7-H3-targeting antibody for pancreatic cancer therapy in mouse models. Nucl Med Biol 2018;58:67–73.
34. Zhou R, Yazdanifar M, Roy LD, Whilding LM, Gavrill A, Maher J, et al. CAR T cells targeting the tumor MUC1 glycoprotein reduce triple-negative breast cancer growth. Front Immunol 2019;10:1149.
35. Morgan SC, Hoffman K, Loblaw DA, Buyyounouski MK, Patton C, Barocas D, et al. Hypofractionated radiation therapy for localized prostate cancer: executive summary of an ASTRO, ASCO, and AUA evidence-based guideline. Pract Radiat Oncol 2018;8:354–60.
36. Saga R, Matsuya Y, Takahashi R, Hasegawa K, Date H, Hosokawa Y. Analysis of the high-dose-range radioresistance of prostate cancer cells, including cancer stem cells, based on a stochastic model. J Radiat Res 2019; 60:298–307.
37. Wang X, Ma Z, Xiao Z, Liu H, Dou Z, Feng X, et al. Chk1 knockdown confers radiosensitization in prostate cancer stem cells. Oncol Rep 2012;28: 2247–54.
38. Chang L, Graham P, Hao J, Ni J, Bucci J, Cozzi P, et al. Acquisition of epithelial–mesenchymal transition and cancer stem cell phenotypes is associated with activation of the PI3K/Akt/mTOR pathway in prostate cancer radioresistance. Cell Death Dis 2013;4:e875.
39. Yu C, Yao Z, Jiang Y, Keller ET. Prostate cancer stem cell biology. Minerva Urol Nefrol 2012;64:19.
40. Ciardiello C, Leone A, Lanuti P, Roca MS, Moccia T, Minciacchi VR, et al. Large oncosomes overexpressing integrin alpha-V promote prostate cancer adhesion and invasion via AKT activation. J Exp Clin Cancer Res 2019:38:317.
41. Deng Z, Wu Y, Ma W, Zhang S, Zhang Y-Q. Adoptive T-cell therapy of prostate cancer targeting the cancer stem cell antigen EpCAM. BMC Immunol 2015;16:1.
42. Weiss T, Weller M, Guckenberger M, Sentman CL, Roth P. NKG2D-based CAR T cells and radiotherapy exert synergistic efficacy in glioblastoma. Cancer Res 2018;78:1031–43.
43. DeSelm C, Palomba ML, Yahalom J, Hamieh M, Eyquem J, Rajasekhar VK, et al. Low-dose radiation conditioning enables CAR T cells to mitigate antigen escape. Mol Ther 2018;26:2542–52.
44. Qu C, Ping N, Kang L, Liu H, Qin S, Wu Q, et al. Radiation priming chimeric antigen receptor T-cell therapy in relapsed/refractory diffuse large B-cell lymphoma with high tumor burden. J Immunother 2020;43:32–7.
45. Wright CM, LaRiviere MJ, Baron JA, Uche C, Xiao Y, Arscott WT, et al. Bridging Radiation therapy before commercial chimeric antigen receptor T-cell therapy for relapsed or refractory aggressive B-cell lymphoma. Int J Radiat Oncol Biol Phys 2020:108:178–88.
46. Minn I, Rowe SP, Pomper MG. Enhancing CAR T-cell therapy through cellular imaging and radiotherapy. Lancet Oncol 2019;20:e443–e51.
47. Reits EA, Hodge JW, Herberts CA, Groothuis TA, Chakraborty M, Wansley EK, et al. Radiation modulates the peptide repertoire, enhances MHC class I expression, and induces successful antitumor immunotherapy. J Exp Med 2006;203:1259–71.
48. Lardas M, Liew M, van den Bergh RC, De Santis M, Bellmunt J, Van den Broeck T, et al. Quality of life outcomes after primary treatment for clinically localised prostate cancer: a systematic review. Eur Urol 2017; 72:869–85.
49. Wallis CJ, Glaser A, Hu JC, Huland H, Lawrentschuk N, Moon D, et al. Survival and complications following surgery and radiation for localized prostate cancer: an international collaborative review. Eur Urol 2018;73:11–20.
50. Smith EL, Mailankody S, Staehr M, Wang X, Senechal B, Purdon TJ, et al. BCMA-targeted CAR T-cell therapy plus radiotherapy for the treatment of refractory myeloma reveals potential synergy. Cancer Immunol Res 2019;7: 1047–53.